Confinement of Equilibrium Polymers: A Field-Theoretic Model and Mean-Field Solution

Edward H. Feng*

College of Chemistry, University of California, Berkeley, Berkeley, California 94720

Glenn H. Fredrickson

Department of Chemical Engineering and Materials, Materials Research Laboratory, University of California, Santa Barbara, Santa Barbara, California 93106

Received October 13, 2005; Revised Manuscript Received December 16, 2005

ABSTRACT: We develop a field-theoretic model for equilibrium polymers in good solvent. Using the Gaussian chain model, we present a derivation in the grand canonical ensemble in which the parameters are the monomer chemical potential μ_M, the excluded volume parameter u_0, and the energy decrease for forming a bond $2h$. Only the quantity Γ, which is proportional to u_0e^{-2h}, matters in determining the mean-field solution. For a bulk system, the homogeneous mean-field solution gives an exponential polymer length distribution with a characteristic length that decreases with increasing Γ. Moreover, the extent of polymer overlap in a semi-dilute solution decreases with increasing density in the mean-field approximation. We study the inhomogeneous properties of equilibrium polymers confined between two parallel repulsive plates with numerical self-consistent field theory. The polymer length distribution is exponential for all L, the dimensionless distance between the plates. For small L, the characteristic polymer length of the exponential distribution scales as L^2, which is ideal equilibrium polymer behavior. For any fixed L, the characteristic length approaches the bulk characteristic length as Γ increases. We also find that α, the ratio of the volume-averaged confined density to the bulk density, decreases monotonically with decreasing Γ and L. As $u_0 \rightarrow 0$, our data converge to previous analytic results for ideal equilibrium polymers.

1. Introduction

An equilibrium polymer system consists of monomers or short oligomers that each have two bonding groups on opposite ends of the molecule. The reaction of two bonding groups on different monomers to form a bond is in chemical equilibrium, so monomers can self-assemble to form linear and cyclic polymers. Figure 1 shows a schematic drawing of an equilibrium polymer system. Examples of equilibrium polymers include DNA tiles[9] and so-called giant micelles[4] which are surfactant systems that form long tubelike micelles that can break and recombine at any point along the micelle. Equilibrium polymers differ from "living polymers" in that reversible polymerization occurs only after an initiation step in the latter.[15] The concentration of initiators greatly affects the thermodynamics of living polymers[6−8] while there is no initiation step for equilibrium polymers.

Recently, Meijer and co-workers made synthetic equilibrium polymers by attaching reversible bonding groups consisting of four hydrogen bonding moieties on both ends of linear oligomers.[22] At a low temperature, the energy of the bonding groups dominated the thermodynamics, which resulted in long polymers. At a high temperature, the system consisted of mostly unbonded oligomers due to the large translational entropy of this system. The viscosity of the solution at these two temperatures differed by orders of magnitude, and temperature could be used to reversibly control the viscosity between these extremes. These initial experiments highlighted the exciting technological opportunities for using these synthetic bonding groups to design polymeric materials whose properties can be tuned with temperature.[2]

If the reversible bonding occurs on an experimental time scale, then an equilibrium polymer system exhibits an annealed polydispersity. The polymer length distribution is determined solely by the chemical equilibrium of the bonding reaction, not by the conditions of the initial synthesis of the polymers. Consider the polymer length distribution of an equilibrium polymer system that does not form cyclic polymers. If the bonding reaction occurs independently of the number of monomers attached to the two bonding monomers, then the polymer length distribution is exponential. This has been predicted by analytic theory[3] as well as confirmed in particle-based simulations[26] and recent experiments using optical microscopy to measure the length distribution of DNA tiles.[9] However, we note that scaling arguments predict nonexponential length distributions in the semi-dilute regime.[26]

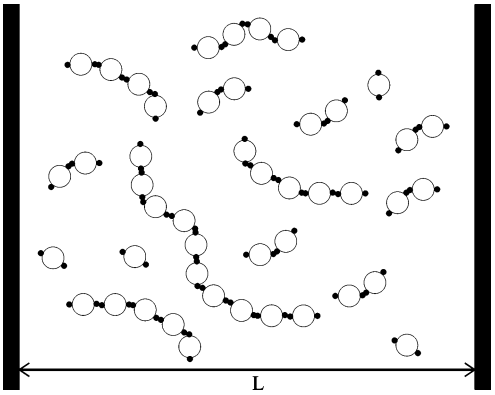

Figure 1. In this schematic drawing of an equilibrium polymer, the large open circles represent monomers while the small filled circles represent bonding groups. The vertical lines symbolize the repulsive walls that confine the equilibrium polymer.

In this paper, we consider the confinement of equilibrium polymers, which is an interesting scientific question that also has potential applications in controlling the aggregation of

* Corresponding author. E-mail: efeng@statmech.org.

10.1021/ma052223l CCC: $33.50
Published on Web 02/22/2006

colloidal dispersions. The literature on confined equilibrium polymers began with Schmitt et al., who provided an analytic mean-field treatment of dilute, ideal polymers between two repulsive parallel plates.[21] van der Gucht, Besseling, and Fleer extended this formalism to account for attractive walls and obtained exact results for numerous quantities including the density profile and average polymer length.[24] These three authors have also developed self-consistent field theories for two distinct models of equilibrium polymers at interfaces.[23,25] Monte Carlo studies of confined equilibrium polymers have been based on a *q*-state Potts model.[17] Milchev and Landau explored the polymer length distribution and density profiles for a fixed width between the plates[18] while Rouault and Milchev studied the dependence of the average polymer length on this width.[19]

Here, we introduce a new field-theoretic model for equilibrium polymers based on the Gaussian chain model for flexible polymers. In this coarse-grained description, the polymer segments interact through an excluded volume potential, and there is an energy of bonding when two monomers form a bond. While previous authors have used field-theoretic models to study equilibrium polymers at interfaces,[25] our model is useful in studying both bulk and interfacial properties and does not assume an exponential length distribution. It is most convenient to derive this model in the grand canonical ensemble. In the mean-field approximation, we give analytic results for a homogeneous bulk system. For equilibrium polymers in confinement, quantities such as the density become inhomogeneous, and numerical methods are needed. We use field-theoretic computer simulations in the mean-field approximation to study the polymer length distribution and the density profile for equilibrium polymers confined between two repulsive parallel plates, the situation depicted schematically in Figure 1.

The paper has the following organization: Section 2 formulates the field-theoretic model and gives expressions for the density and polymer length distribution. We develop the mean-field solution for a homogeneous bulk system and devise scaling arguments for confined equilibrium polymers in section 3, while section 4 outlines the numerical methods used to study equilibrium polymers confined between two repulsive parallel plates. We show our results for confined equilibrium polymers in section 5 and conclude with a discussion of future uses for this model in section 6.

2. Equilibrium Polymer Model

We formulate a discrete Gaussian chain model for equilibrium polymers in the grand canonical ensemble with fixed monomer chemical potential μ_M, volume V, and temperature T. A state of the system is described by the positions and momenta of n_M monomers and their connectivity into linear polymers; we exclude ring formation in our model for simplicity. The connectivity is described by $\{n(N_B)\} \equiv \{n(1), n(2), ..., n(n_M)\}$, a set of nonnegative integers that gives the number of polymers with $N_B = 1, 2, ..., n_M$ monomers. Each monomer along a polymer corresponds to a bead in the discrete Gaussian chain model, and the spring between two bonded monomers has a harmonic stretching energy. The grand canonical partition function is

$$\Xi(\mu_M,V,T) = \sum_{n_M=0}^{\infty} \frac{1}{n_M!} \sum_{\{n(N_B)\}}^{*} \int d\mathbf{r}_1 ... d\mathbf{r}_{n_M} \times C(n_M;\{n(N_B)\}) e^{-U_0(n_M;\{n(N_B)\})-(u_0/2)\int \hat{\rho}(\mathbf{r})^2 d\mathbf{r}-2hn_P} \frac{e^{\mu_M n_M}}{\lambda_T^{3n_M}} \quad (1)$$

where $\mathbf{r}_i$ denotes the position of the i monomer and the starred summation over $\{n(N_B)\}$ implies a summation over all sets of nonnegative integers $n(1)$, $n(2)$, ..., $n(n_M)$ such that

$$\sum_{N_B=1}^{n_M} N_B n(N_B) = n_M \quad (2)$$

Also,

$$C(n_M;\{n(N_B)\}) = \frac{n_M!}{n(1)!n(2)!\cdots n(n_M)!}$$

is the number of ways of arranging n_M distinguishable monomers into $n(1)$ indistinguishable monomers, $n(2)$ indistinguishable dimers, $n(3)$ indistinguishable polymers with three monomers, etc., and $U_0(n_M;\{n(N_B)\})$ is the harmonic potential for a configuration in which the first $n(1)$ monomers are unbonded, the next $2n(2)$ monomers form dimers, etc. For example

$$U_0(3;\{0,0,1\}) = \frac{3}{2b^2}|\mathbf{r}_1 - \mathbf{r}_2|^2 + \frac{3}{2b^2}|\mathbf{r}_2 - \mathbf{r}_3|^2 \quad (3)$$

for a system with three monomers that form a polymer with three monomers. Here, b is the root-mean-square length between two bonded monomers. For each possible $\{n(N_B)\}$, we write down a configuration integral for one arrangement of monomers and then multiply by $C(n_M;\{n(N_B)\})$ to account for all possible ways that n_M monomers can form a set of polymers described by $\{n(N_B)\}$ in which polymers of the same length are indistinguishable. We also include an excluded volume potential parametrized by $u_0 > 0$ for a good solvent; the microscopic density is

$$\hat{\rho}(\mathbf{r}) = \sum_{i=1}^{n_M} \delta(\mathbf{r} - \mathbf{r}_i)$$

Also, there is an energy h in units of kT for each unsatisfied bonding group, which models the chemical equilibrium of the bond formation reaction. While $h > 0$ implies a decrease in energy upon bonding, this parameter can be any real number. This bonding energy is proportional to the number of polymers

$$n_P = \sum_{N_B=1}^{\infty} n(N_B) \quad (4)$$

Lastly, λ_T is the de Broglie wavelength that arises from a one-dimensional momentum integration.

We decouple the excluded volume interactions with a standard Hubbard−Stratonovich transformation; this introduces a functional integral over $w(\mathbf{r})$, a chemical potential field conjugate to the density. Also, we replace the two discrete summations in eq 1 with summations over the number of polymers with N_B monomers:

$$\sum_{n_M=1}^{\infty} \sum_{\{n(N_B)\}}^{*} \leftrightarrow \sum_{n(1),n(2),...=0}^{\infty}$$

Since the starred summation implies eq 2, it is straightforward to show the equivalence of the two sets of summations. Using eqs 4 and 2, the partition function becomes

$$\Xi(\mu_M,V,T) = \sum_{n(1),n(2),\ldots=0}^{\infty} \frac{1}{n(1)!n(2)!\cdots}\int \mathscr{D}w e^{-1/(2u_0)\int w(\mathbf{r})^2 d\mathbf{r}} \times \prod_{N_B=1}^{\infty}\left(e^{-2h}\left(\frac{e^{\mu_M}}{\lambda_T^3}\right)^{N_B} Q_0(N_B)Q(N_B;[iw])\right)^{n(N_B)} \quad (5)$$

where $\int \mathscr{D}w$ denotes a functional integration over the $w(\mathbf{r})$ field and

$$Q(N_B;[iw]) = Q_0(N_B)^{-1}\int d\mathbf{r}_1 \ldots d\mathbf{r}_{N_B} e^{-U_0(N_B;\{0,0,\ldots,n(N_B)=1\})-\sum_{i=1}^{N_B} iw(\mathbf{r}_i)}$$

is the normalized single chain partition function of a polymer with N_B monomers in an external field $iw(\mathbf{r})$ such that $Q(N_B;[0]) = 1$. The normalization factor is

$$Q_0(N_B) = \int d\mathbf{r}_1 \ldots d\mathbf{r}_{N_B} e^{-U_0(N_B;\{0,0,\ldots,1\})} = V g_M{}^{N_B-1}$$

where $g_M = (2\pi b^2/3)^{3/2}$ for the discrete Gaussian chain model. The factor $(n(1)!n(2)!\cdots)^{-1}$ in eq 5 accounts for the indistinguishability of the polymers of the same length. Performing the summations over $n(N_B)$ for $N_B = 1, 2, \ldots$ gives

$$\Xi(\mu_M,V,T) = \int \mathscr{D}w e^{-\mathscr{H}[w]}$$

where the effective Hamiltonian is

$$\mathscr{H}[w] = \frac{1}{2u_0}\int w(\mathbf{r})^2 d\mathbf{r} - e^{-2h}\frac{V}{g_M}\sum_{N_B=1}^{\infty} z_M{}^{N_B} Q(N_B;[iw])$$

and $z_M \equiv (g_M/\lambda_T{}^3)e^{\mu_M}$ is a dimensionless monomer activity.

Consider a polymer with N monomers. To this point, we have used a discrete Gaussian chain with $N_B = N$ beads to describe this polymer. It is also possible to represent this polymer with a discrete chain of $N_B \gg N$ beads. In the limit as $N_B \to \infty$, while matching the radii of gyration of the model and real chains, we obtain the continuous Gaussian chain model in which a continuous space curve represents a polymer of length N. For our equilibrium polymer model, the effective Hamiltonian becomes

$$\mathscr{H}[w] = \frac{1}{2u_0}\int w(\mathbf{r})^2 d\mathbf{r} - e^{-2h}\frac{V}{g_M}\int_0^{\infty} dN\, z_M{}^N Q(N;[iw]) \quad (6)$$

where the single chain partition function is now the path integral

$$Q(N;[iw]) = \frac{\int \mathscr{D}\mathbf{R}_N e^{-U_0(\mathbf{R}_N)-\int_0^N iw(\mathbf{R}_N(s))ds}}{\int \mathscr{D}\mathbf{R}_N e^{-U_0(\mathbf{R}_N)}} \quad (7)$$

where $\mathbf{R}_N(s)$ denotes a position $s \in [0, N]$ on a continuous space curve of a polymer of length N, the functional integration is over all possible space curves, and $U_0(\mathbf{R}_N) = (3/(2b^2))\int_0^N |d\mathbf{R}_N(s)/ds|^2\, ds$ is the harmonic stretching energy. Since the normalization factor $Q_0(N) = \int \mathscr{D}\mathbf{R}_N e^{-U_0(\mathbf{R}_N)}$ scales linearly with the volume, we express it as $Q_0(N) = V g_M{}^{N-1}$ where g_M is a monomer volume independent of N and V. One can show that

$$Q(N;[iw]) = \frac{1}{V}\int q(\mathbf{r},N;[iw])\, d\mathbf{r}$$

where $q(\mathbf{r},N;[iw])$ is obtained by solving the complex diffusion equation

$$\frac{\partial}{\partial s}q(\mathbf{r},s;[iw]) = \frac{b^2}{6}\nabla^2 q(\mathbf{r},s;[iw]) - iw(\mathbf{r})q(\mathbf{r},s;[iw])$$

with the initial condition $q(\mathbf{r},0;[iw]) = 1$. One of us gives an alternative derivation of this continuous Gaussian chain model for equilibrium polymers elsewhere.[11]

Observables in this field theoretic model are obtained by functional integrals over the complex field $w(\mathbf{r})$ of the appropriate functionals

$$\langle \mathscr{A} \rangle = \frac{\int \mathscr{D}w \mathscr{A}[w] e^{-\mathscr{H}[w]}}{\int \mathscr{D}w e^{-\mathscr{H}[w]}} \quad (8)$$

where $\langle \mathscr{A} \rangle$ is the ensemble average of an observable and $\mathscr{A}[w]$ is the corresponding functional. For the continuous Gaussian chain model, one can show that the functional for the total monomer density is

$$\rho(\mathbf{r};[iw]) = \frac{e^{-2h}}{g_M}\int_0^{\infty} dN\, z_M{}^N \int_0^N q(\mathbf{r},s;[iw])\, q(\mathbf{r},N-s;[iw])\, ds$$

so then

$$\rho(\mathbf{r},N;[iw]) = \frac{e^{-2h}}{g_M} z_M{}^N \int_0^N q(\mathbf{r},s;[iw])\, q(\mathbf{r},N-s;[iw])\, ds$$

is the contribution to the total monomer density from polymers of length N. The functional for the polymer length distribution

$$p(N;[iw]) = \frac{1}{NV}\int \rho(\mathbf{r},N;[iw])\, d\mathbf{r} = \frac{e^{-2h}}{g_M} z_M{}^N Q(N;[iw])$$

gives the number density of polymers of length N. This distribution is not necessarily exponential in N. Similar functional expressions for the density and polymer length distribution can be derived for the discrete Gaussian chain model of equilibrium polymers.

3. Analytic Results

3.1. Mean-Field Solution for Bulk System. For small u_0, the quadratic term in eq 6 constrains $w(\mathbf{r})$ to a narrow harmonic well near zero for all $\mathbf{r}$. In the limit as $u_0 \to 0$, $w(\mathbf{r}) \approx 0$ for all $\mathbf{r}$, so $Q(N;[0]) = 1$. Then the polymer length distribution

$$p(N;[0]) \sim z_M{}^N Q(N;[0]) = \exp(-[-\ln z_M]N) \quad (9)$$

is exponential for the physically relevant values $z_M \in (0, 1)$. We define $N_0 \equiv -(\ln z_M)^{-1}$ as the characteristic polymer length for an ideal equilibrium polymer. We express all position vectors $\mathbf{x} \equiv \mathbf{r}/R_{g0}$ in units of $R_{g0} = (N_0/6)^{1/2}b$, the ideal radius of gyration of an average polymer, and define a scaled field $W(\mathbf{x}) \equiv N_0 w(\mathbf{x})$. The Hamiltonian becomes

$$\mathscr{H}[W] = \frac{R_{g0}{}^3}{2u_0 N_0{}^2}\int W(\mathbf{x})^2 d\mathbf{x} - e^{-2h}\frac{V}{g_M}N_0\int_0^{\infty} e^{-l}Q(l;[iW])\, dl$$

where $l \equiv N/N_0$.

In this paper, we consider mean-field solutions that require finding the saddle point $W^*(\mathbf{x})$ that satisfies

$$\frac{1}{{R_{g0}}^3}\frac{\delta \mathscr{H}[W]}{\delta W(\mathbf{x})}\bigg|_{W^*(\mathbf{x})} = \frac{W^*(\mathbf{x})}{{u_0}{N_0}^2} + i\frac{\rho(\mathbf{x};[iW^*])}{N_0} = 0 \quad (10)$$

Since we are only interested in physically relevant saddle points that give a real valued density, eq 10 implies that $W^*(\mathbf{x})$ must be purely imaginary. Hence, we define a real field $P(\mathbf{x}) \equiv iW(\mathbf{x})$, and the mean-field equation becomes

$$\frac{1}{{R_{g0}}^3}\frac{\delta \mathscr{H}[P]}{\delta P(\mathbf{x})}\bigg|_{P^*(\mathbf{x})} = -\frac{P^*(\mathbf{x})}{{u_0}{N_0}^2} + \frac{\rho(\mathbf{x};[P^*])}{N_0} = 0 \quad (11)$$

where the total density is

$$\rho(\mathbf{x};[P]) = \frac{\mathrm{e}^{-2h}}{g_M}{N_0}^2\int_0^\infty \mathrm{e}^{-l}\left(\int_0^l q(\mathbf{x},t;[P])\, q(\mathbf{x},l-t;[P])\, \mathrm{d}t\right)\mathrm{d}l \quad (12)$$

with $t \equiv s/N_0$ and the propagator satisfies the modified diffusion equation

$$\frac{\partial}{\partial t}q(\mathbf{x},t;[P]) = \nabla^2 q(\mathbf{x},t;[P]) - P(\mathbf{x})\, q(\mathbf{x},t;[P]) \quad (13)$$

with the initial condition $q(\mathbf{x},0;[P]) = 1$. The real valued nature of $P(\mathbf{x})$ and the initial condition imply that $q(\mathbf{x},t;[P])$ is real for all $\mathbf{x}$ and t, so then $\rho(\mathbf{x};[P])$ is real for all $\mathbf{x}$. Combining eqs 11 and 12 into

$$P^*(\mathbf{x}) = \Gamma\int_0^\infty \mathrm{e}^{-l}\left(\int_0^l q(\mathbf{x},t;[P^*])\, q(\mathbf{x},l-t;[P^*])\, \mathrm{d}t\right)\mathrm{d}l \quad (14)$$

shows that only the dimensionless parameter $\Gamma \equiv (u_0/g_M)\mathrm{e}^{-2h}N_0^3$ matters in determining the mean-field solution for this equilibrium polymer model. Once we use this mean-field equation to find the saddle point $P^*(\mathbf{x})$, we can calculate the monomer density from one polymer length

$$\rho(\mathbf{x},l;[P]) = \frac{\mathrm{e}^{-2h}}{g_M}{N_0}^2\mathrm{e}^{-l}\int_0^l q(\mathbf{x},t;[P])\, q(\mathbf{x},l-t;[P])\, \mathrm{d}t \quad (15)$$

and the polymer length distribution

$$p(l;[P]) \sim \mathrm{e}^{-l}Q(l;[P]) \quad (16)$$

where

$$Q(l;[P]) = \frac{{R_{g0}}^3}{V}\int q(\mathbf{x},l;[P])\, \mathrm{d}\mathbf{x}$$

is the single chain partition function.

For this field-theoretic model subject to periodic boundary conditions, there exists a homogeneous saddle point $P^*(\mathbf{x}) = P_h$ independent of $\mathbf{x}$ which corresponds to the mean-field solution for a bulk system. The position independent nature of this saddle point implies $q(\mathbf{x},s;[P_h]) = \exp(-P_h s)$, which gives

$$\rho_0 \equiv \rho(\mathbf{x};[P_h]) = \frac{\mathrm{e}^{-2h}}{g_M}\frac{{N_0}^2}{(1+P_h)^2} \quad (17)$$

for the bulk density. Equation 11 becomes $P_h = u_0\rho_0 N_0$, which implies that P_h must satisfy the cubic equation

$$P_h^3 + 2P_h^2 + P_h - \Gamma = 0 \quad (18)$$

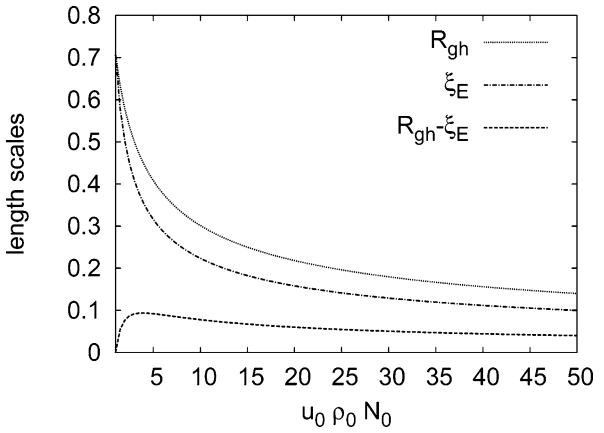

Figure 2. Plot of the radius of gyration of a polymer of average length R_{gh}, the Edwards correlation length ξ_E, and $R_{gh} - \xi_E$ in units of R_{g0} for $u_0\rho_0 N_0 \geq 1$. The length $R_{gh} - \xi_E$, a measure of polymer overlap, exhibits a maximum at $u_0\rho_0 N_0 \approx 3.85$.

Since $\Gamma \equiv (u_0/g_M)\mathrm{e}^{-2h}N_0^3 > 0$ for good solvent conditions, one can prove there exists a unique real root $P_h > 0$. The bulk polymer length distribution

$$p_h(l) \sim \mathrm{e}^{-l}Q(l;[P_h]) = \mathrm{e}^{-(1+P_h)l}$$

is exponential with a characteristic length $l_h = (1 + u_0\rho_0 N_0)^{-1}$ in units of N_0. Since $u_0\rho_0 N_0 > 0$, this field-theoretic model with excluded volume always gives a bulk characteristic length shorter than the ideal characteristic length. Moreover, the characteristic length decreases with increasing excluded volume parameter and density. This is strikingly different from a solution of fixed length homopolymers in which chain length is independent of these two parameters.

We consider scaling predictions of this bulk mean-field solution in two regimes. If $u_0\rho_0 N_0 \ll 1$, $l_h \approx 1$ so the unscaled characteristic length $\langle N\rangle \approx N_0$ is determined by z_M. In this regime of dilute, ideal equilibrium polymers, eq 17 implies the scaling

$$\langle N\rangle \approx N_0 \sim (\rho_0 g_M)^{1/2}\mathrm{e}^h \quad (19)$$

which has been derived previously by other mean-field arguments.[26] If $u_0\rho_0 N_0 \gg 1$, $l_h \sim (u_0\rho_0 N_0)^{-1}$ and $\rho_0 \sim \mathrm{e}^{-2h}l_h^2$ give the scaling

$$l_h \sim \Gamma^{-1/3} = \left(\frac{u_0}{g_M}\right)^{-1/3}\mathrm{e}^{2h/3}N_0^{-1} \quad (20)$$

for the bulk characteristic chain length.

Since the characteristic polymer length changes with excluded volume parameter and density, the physical picture of polymer overlap in a semi-dilute solution of equilibrium polymers is different from a solution of fixed length homopolymers. The ideal radius of gyration for a polymer of length l_h defines a length scale $R_{gh} = (1 + u_0\rho_0 N_0)^{-1/2}$ in units of R_{g0}, and we compare this with the Edwards correlation length $\xi_E = (2u_0\rho_0 N_0)^{-1/2}$ in units of R_{g0}. The condition $u_0\rho_0 N_0 = 1$ denotes a crossover from a dilute to a semi-dilute solution in which polymers overlap. We plot R_{gh} and ξ_E as well as $R_{gh} - \xi_E$ in the semidilute regime in Figure 2. The difference between these two length scales provides a measure of polymer overlap that shows a peak at $u_0\rho_0 N_0 = 4^{1/3}/(2 - 4^{1/3}) \approx 3.85$. As $u_0\rho_0 N_0$ increases, the mean-field approximation predicts that both length scales converge to zero, so the system becomes a melt of primarily monomers. We note that a length scale similar to R_{gh}

has appeared in the analysis of a field-theoretic model that considers equilibrium polymers near an interface.[25]

3.2. Scaling Arguments for Confinement. For an equilibrium polymer confined between two repulsive plates, we develop arguments for how the characteristic polymer length scales with L, the dimensionless distance between the plates in units of R_{g0}. While the results in this section have been stated previously,[21] we present an alternative, simpler argument for these scaling relations. Moreover, these scaling relations will help in understanding our numerical results. For a dilute, ideal system, we assume a free energy density in units of kT of

$$F = N_0 \int_0^\infty p(l) \ln[p(l)b^3] \, dl + N_0 \int_0^\infty 2hp(l) \, dl + F_C$$

where the terms to the right of the equality correspond to translational entropy, energy of bonding, and the confinement free energy F_C, respectively.[21] For an ideal system, F_C includes only a confinement entropy, which scales as $(N/N_0)L^{-2}$ for a polymer of length N.[5] In this case the confinement entropy for a system of equilibrium polymers is

$$F_C = N_0 \int_0^\infty \frac{l}{L^2} p(l) \, dl$$

We determine the distribution $p^*(l)$ that minimizes F with respect to the constraint

$$\rho_0 = N_0^2 \int_0^\infty l p(l) \, dl \tag{21}$$

using a Lagrange multiplier method

$$p^*(l) \sim e^{-2h - \lambda N_0 l - l/L^2}$$

where λ is the Lagrange multiplier. For a bulk system in which $L \gg 1$, the confinement entropy is negligible and the bulk characteristic length is $l_h = 1/(\lambda N_0)$. Satisfying the constraint in eq 21 implies the scaling relation in eq 19. The inclusion of the confinement entropy gives a confined characteristic length $l_c = l_h/(1 + l_h L^{-2})$. For an ideal equilibrium polymer in confinement, the polymer length distribution remains exponential with a shorter characteristic length. For strong confinement in which $L \ll 1$, we obtain the scaling relation

$$l_c \sim L^2 \tag{22}$$

This implies that the radius of gyration of an ideal polymer with average size $R_g \sim l_c^{1/2} \sim L$ scales linearly with the confinement length, which provides a physical picture of confinement in which the average of the exponential distribution changes so that a polymer of average length fits between the plates.

Now consider a dilute system in good solvent. Since each chain exhibits excluded volume statistics, the confinement entropy of a polymer of length N scales as $(N/N_0^{5/6})L^{-5/3}$ so then

$$F_C \sim \int_0^\infty \frac{l}{L^{5/3}} p(l) \, dl$$

Repeating our previous analysis gives the scaling relation

$$l_c \sim L^{5/3}$$

so in tight confinement the radius of gyration of an average polymer with excluded volume statistics, $R_g \sim l_c^{3/5} \sim L$, scales linearly with the confinement length. While we have neglected a repulsive energy proportional to ρ_0^2, we obtain the same physical picture of equilibrium polymer confinement as in the ideal situation. We also expect this scaling relation to hold for semi-dilute solutions in which $L < \xi$, where ξ is the mesh or "blob" length. In this regime, the behavior will be dominated by single chains with excluded volume statistics.

4. Numerical Methods for Confined System

When an equilibrium polymer is confined between two repulsive parallel plates, observables such as the density become inhomogeneous, and numerical methods are necessary to find the solutions to eq 11. In the mean-field approximation for this geometry, we assume that quantities such as $P(\mathbf{x})$ are constant in the two dimensions parallel to the plates and perform a one dimensional calculation in the perpendicular dimension. If x is a dimensionless scalar length perpendicular to the plates, we model the effect of two repulsive plates at $x = 0, L$ by imposing Dirichlet boundary conditions on the propagator

$$q(x,t;[P]) = 0$$

for $x = 0$, L and $t \geq 0$. These boundary conditions also imply that the densities in eqs 12 and 15 vanish at the plates. Physically, the plates correspond to an infinite potential outside the region $x \in (0, L)$ that forbids the equilibrium polymer from escaping this region. Moreover, formulating this model for confined equilibrium polymers in the grand canonical ensemble implies that the confined system can exchange particles with a bulk reservoir with the properties described in section 3.1.

We begin each simulation by choosing initial values for $P(x)$. Since the mean-field solution $P^*(x)$ scales linearly with the density that looks roughly sinusoidal in previous calculations on confined polymers,[1] we set $P(x) \sim \sin(\pi x/L)$. The diffusion equation in eq 13 is solved with a pseudo-spectral algorithm described elsewhere.[11] To implement this algorithm, we represent the propagator and other functions of x at discrete points

$$q_i(t;[P]) \equiv q(iL/(M+1),t;[P])$$

for $i = 1, 2, ..., M$ and employ the fast sine transform in the *fftw* packages[14] to obtain a spectral representation of the propagator

$$a_k(t;[P]) = 2\sum_{i=1}^{M} q_i(t;[P]) \sin\left(\frac{k\pi i}{M+1}\right)$$

where we use $M = 255$. Because of the polydispersity of the equilibrium polymer, one would ideally solve for $q(x,t;[P])$ for all $t \geq 0$. But since $t = 1$ corresponds to the bulk characteristic polymer length and we expect a shorter average length in confinement, we solve for the propagator in the interval $t \in [0, 5]$ with a contour step size $\Delta t = 0.005$. Calculations with larger intervals give the same results.

We calculate the density in eq 12 using Simpson's rule to evaluate the quadratures over the polymer length l. This allows us to evaluate $\delta\mathscr{H}[P]/\delta P(x)$ with eq 11 and update the field according to

$$P_{j+1}(x) = P_j(x) + \zeta \left.\frac{\delta\mathscr{H}[P]}{\delta P(x)}\right|_{P_j(x)} \tag{23}$$

where the subscripts on the field denote the iteration step and $\zeta > 0$ is an arbitrary relaxation parameter. This succession of fields is simply a method of finding the inhomogeneous saddle

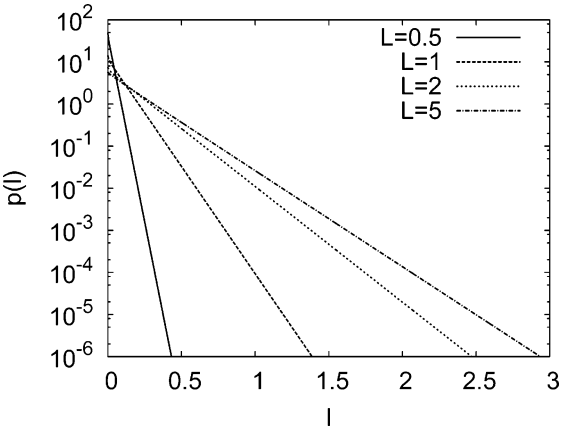

Figure 3. A semi-log plot of the polymer length distribution for $N_0 = 50$ and $\Gamma = 100$ for different confinement lengths L. The distributions are all exponential, and the characteristic length decreases as L decreases.

point and does not correspond to any physical dynamics. Each new field requires the calculations described in the previous paragraph to calculate eq 11, and we iterate this process until a field $P^*(x)$ satisfies the error criteria that the average value of $|\delta\mathscr{F}[P]/\delta P(x)|$ is less than 10^{-4}. Note that formulating our self-consistent field theory in terms of a real field $P(x)$ instead of a complex field $W(x)$ reduces the saddle point search space by half. With this inhomogeneous saddle point, we use

$$Q(l;[P]) = \frac{2}{\pi(M+1)} \sum_{k=1,3,5\ldots} \frac{a_k(l;[P^*])}{k}$$

to determine the polymer length distribution from eq 16. We calculate the characteristic length using

$$\langle l \rangle = \frac{\int_0^\infty l p(l;[P^*])\, \mathrm{d}l}{\int_0^\infty p(l;[P^*])\, \mathrm{d}l}$$

and the total and one length densities using eqs 12 and 15, respectively. We use Simpson's rule to evaluate the quadratures over l, rather than the Gauss−Laguerre quadrature over the interval $[0,\infty)$ employed in previous studies of polydispersity.[13] Another quantity of interest is

$$\alpha \equiv \frac{1}{\rho_0 L} \int_0^L \rho(x;[P^*])\, \mathrm{d}x \qquad (24)$$

the ratio of the average density between the plates and the bulk density.

5. Confinement Results

For all numerical results, we set $N_0 = 50$. While only Γ matters in determining the bulk mean-field properties of this model, we must specify N_0 in confinement since we express L in units of $R_{g0} = (N_0/6)^{1/2}b$. First, we consider the polymer length distribution, examples of which are shown in Figure 3. For all systems considered in this study, we find exponential length distributions in the mean-field approximation. This is consistent with previous particle simulations.[18] Physically, the repulsive walls do not affect the statistically independent way in which monomers can form linear polymers. With this simple polymer length distribution, it suffices to consider the confined characteristic length l_c for each system.

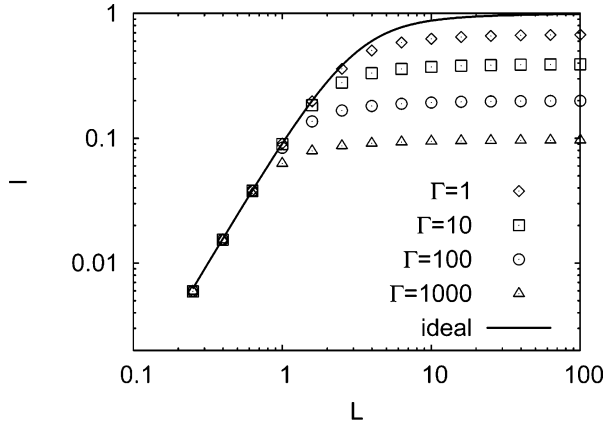

Figure 4. A log−log plot of the characteristic polymer length l vs confinement length L for $N_0 = 50$. The discrete symbols are confined systems for various values of Γ, and the solid line is the analytic prediction of Schmitt et al. in eq 25 for dilute, ideal equilibrium polymers confined between two repulsive parallel plates.[21] The bulk characteristic lengths are 0.682 for $\Gamma = 1$, 0.393 for $\Gamma = 10$, 0.200 for $\Gamma = 100$, and 0.0967 for $\Gamma = 1000$.

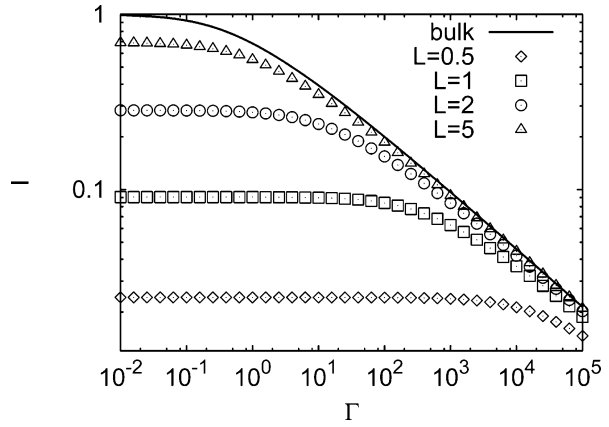

Figure 5. A log−log plot of the characteristic polymer length l vs Γ for $N_0 = 50$. The discrete symbols are confined systems for various values of L, and the solid line is the bulk characteristic length obtained through the solution of eq 18.

We investigate l_c as a function of L for various values of Γ in Figure 4. At small L, the characteristic length is independent of Γ and scales as $l_c \sim L^2$, ideal equilibrium polymer behavior. Moreover, the data in this regime match the analytic prediction of Schmitt et al. for dilute, ideal equilibrium polymers between two repulsive parallel plates[21]

$$l_c^{\mathrm{id}} = \frac{1 - (3/L)\tanh(L/2) + \cosh^{-2}(L/2)/2}{1 - (2/L)\tanh(L/2)} \qquad (25)$$

Later, we present data that show the density in confinement is low enough for small L to expect dilute behavior. In all of our calculations, we do not observe the scaling $l_c \sim L^{5/3}$ for excluded volume statistics because the mean-field approximation does not account for density correlations between monomers from different parts of the same chain. As L becomes large, l_c approaches the bulk characteristic length l_h for each value of Γ. Also, our numerical data approach the ideal equilibrium polymer prediction in eq 25 as the excluded volume parameter u_0 becomes small, which corresponds to $\Gamma \to 0$. The data in Figure 4 are qualitatively consistent with previous particle simulations.[19]

Figure 5 shows how l_c varies with Γ for different values of L. For large Γ, the characteristic length approaches the bulk

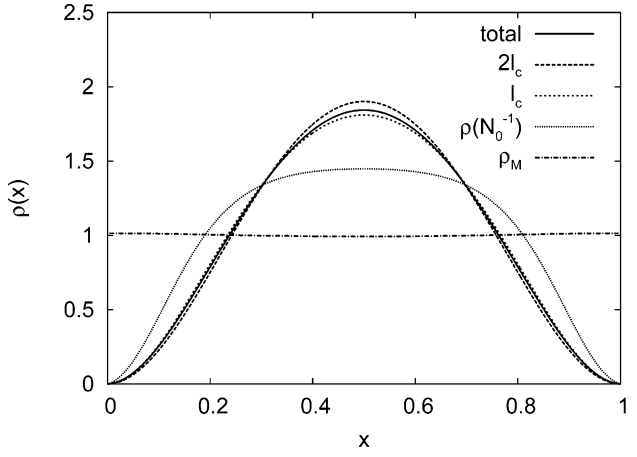

Figure 6. Plot of density profiles for polymers of various length for $N_0 = 50$, $L = 1$, and $\Gamma = 100$. The line labeled $\rho(N_0^{-1})$ corresponds to the monomer density in eq 12, and the line labeled ρ_M is the density for a particle in an external field given in eq 26. The area under each density profile is 1.

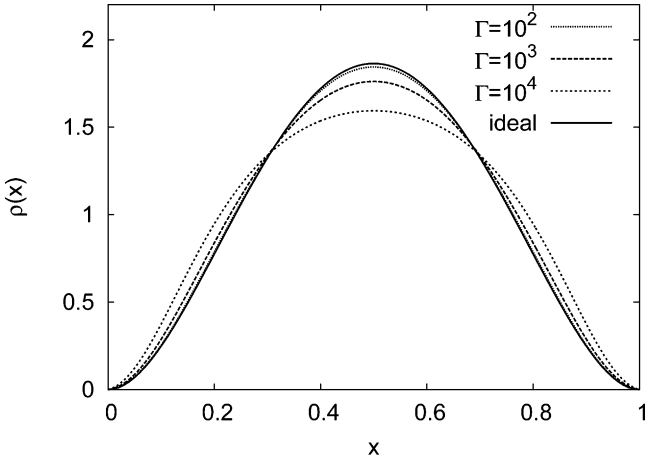

Figure 7. Plot of the density profiles for $N_0 = 50$ and $L = 1$ for various values of Γ. The solid line indicates the analytic result of van der Gucht et al. in eq 27 for dilute, ideal equilibrium polymer.[24] The area under each density profile is 1.

characteristic length given by the solid line. Large Γ implies either large excluded volume potential or a large energy increase upon bonding, both of which lead to short characteristic lengths. For each L, Γ approaches a value such that the radius of gyration of the bulk equilibrium polymer becomes much smaller than L. In this regime, the confined equilibrium polymer does not feel the effect of the plates and behaves like a bulk system. For small Γ, the bulk characteristic length approaches 1 due to either a small excluded volume potential or a large energy decrease upon bonding. In confinement, l_c does not reach this bulk characteristic length and instead approaches a limiting value for each L.

We now consider the inhomogeneous density profiles for confined equilibrium polymers. For comparison purposes, we normalize each profile so that the area under it is 1. Figure 6 shows the profiles for polymers of different length for $L = 1$ and $\Gamma = 100$. The profile is narrowest for polymers of length $2l_c$, where $l_c = 0.089$ for this system. This narrow profile results from the high conformational entropy for long polymers to reside near the wall. Polymers of length l_c feel less of an entropy penalty, which results in a wider density profile. For unbonded monomers in the system, we show $\rho(x,N_0^{-1};[P^*])$ from eq 15 with the dotted line. Physically, we expect an enhanced monomer density near the wall since monomers do not feel the same entropic force as long polymers. However, an entropic depletion of the monomer density is observed due to the Dirichlet boundary conditions imposed on the propagator. There are also inherent errors in representing a monomer as a very short Gaussian chain. An alternative for the monomer density is the density of a single particle in an external field[11]

$$\rho_M(x;[P^*]) = e^{-P^*(x)/N_0} \tag{26}$$

Near the wall, we view this density profile as the limiting behavior as $x \to 0$, L which drops discontinuously to zero at $x = 0$, L. This profile shows a monomer enrichment near the wall, behavior which qualitatively agrees with particle simulations.[18] Moreover, the mean-field equation in eq 11 implies the physically reasonable result that this enrichment becomes more pronounced as the density increases.

For $L = 1$, Figure 7 shows the normalized total density from eq 12 for various values of Γ. Since large Γ implies shorter characteristic lengths, we obtain wider profiles for large Γ due to the smaller conformational entropy penalty for shorter polymers. As Γ becomes small, the density profile approaches the analytic result of van der Gucht et al.

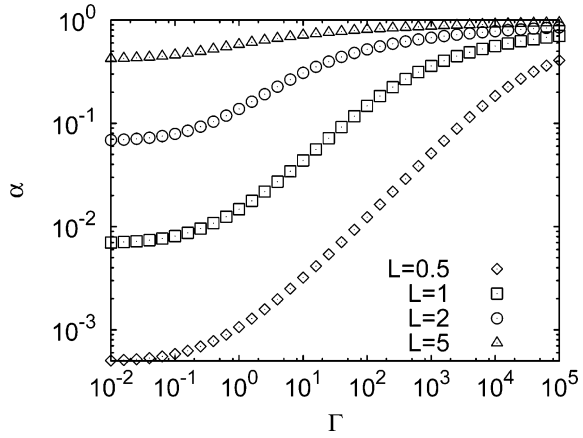

Figure 8. A log−log plot of α, the ratio of the volume averaged confined density to the bulk density, versus Γ for $N_0 = 50$. The discrete symbols are confined systems for various values of L.

$$\frac{\rho^{id}(x)}{\rho_0} = \left(1 - \frac{\cosh(x - (L/2))}{\cosh(L/2)}\right)^2 \tag{27}$$

for a dilute, ideal equilibrium polymer confined between repulsive parallel plates.[24] The previous equation corresponds to their result for the density profile as $C \to \infty$ since C^{-1} is the dimensionless length scale for the surface attraction. To compare the unnormalized total density for different Γ, we plot α, the ratio of the volume-averaged confined density to the bulk density given in eq 24, versus Γ for different L in Figure 8. As Γ decreases, α decreases monotonically, implying that density shifts from the confined region to the bulk reservoir. This occurs because small Γ encourages the formation of long polymers that feel a conformational entropy penalty in confinement. As Γ increases, α approaches 1 for all L since unbonded monomers and short polymers are equally likely to exist between the plates as in a bulk reservoir.

Lastly, we consider α as a function of L for different Γ in Figure 9. Large L corresponds to a bulk system, so $\alpha \to 1$ as $L \to \infty$. As L decreases, α decreases as polymers are squeezed out into the bulk reservoir. For $L \leq 0.5$, the average density in confinement is at least an order of magnitude less than the bulk density, so it is reasonable that the analytic prediction for dilute

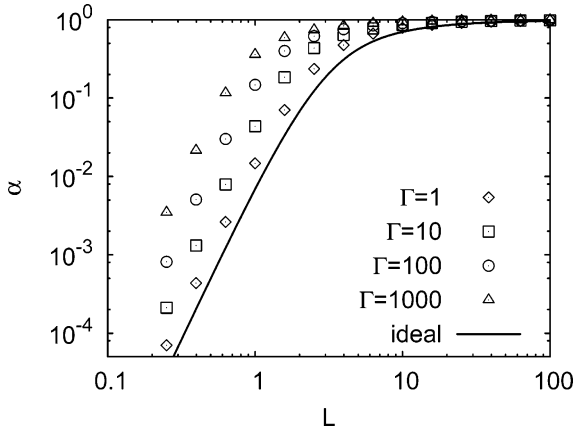

Figure 9. A log−log plot of α, the ratio of the volume averaged confined density to the bulk density, versus L for $N_0 = 50$. The discrete symbols are confined systems for various values of Γ, and the solid line is the analytic prediction of Schmitt et al. in eq 28 for dilute, ideal equilibrium polymers.[21]

equilibrium polymers in eq 25 corresponds to the numerical data in Figure 4. As $\Gamma \to 0$, our data approach the analytic result

$$\alpha^{id} = 1 - (3/L)\tanh(L/2) + (1/2)\cosh^{-2}(L/2) \quad (28)$$

of Schmitt et al. for an ideal equilibrium polymer.[21] This result corresponds to the volume average over the confinement region of the density profile in eq 27.

6. Conclusion and Discussion

We have formulated a field-theoretic model for equilibrium polymers with excluded volume using the Gaussian chain model. Our formalism can be readily extended to treat equilibrium polymers that form rings. The numerical treatment of the inhomogeneous properties of ring-forming systems, however, requires the evaluation of a two-point propagator that is considerably more expensive to evaluate. Other possible variants of this theory include using the wormlike chain model[11] to investigate semiflexible equilibrium polymers. Moreover, the energy of bonding model for chemical equilibrium and grand canonical framework will be useful in formulating models of other supramolecular systems in which reversible bonding influences the thermodynamics. One interesting example is a three component graft copolymer system in which different microphase separated morphologies can be accessed with temperature.[20] Field-theoretic models of such systems can aid in designing materials with unique temperature-dependent properties.

In the mean-field approximation for our equilibrium polymer model, we find an exponential length distribution in the bulk homogeneous phase with a characteristic length that decreases with increasing excluded volume parameter and density. Also, the extent of polymer overlap in a semi-dilute solution of equilibrium polymers decreases with increasing density in the mean-field approximation. In strong confinement, equilibrium polymers are ideal due to the low density between the plates. For any confinement length, the characteristic length approaches the bulk characteristic length as either the excluded volume parameter becomes large or the energy increase upon bonding becomes large. As the excluded volume parameter becomes small, our numerical data approach the analytic predictions for dilute, ideal equilibrium polymers confined between two parallel repulsive plates.[21,24]

We anticipate that this field-theoretic model will be useful in studying other aspects of equilibrium polymers. An exciting possibility is going beyond the mean-field approximation and sampling the field theory with Monte Carlo or complex Langevin methods.[11,12] In a bulk system, these calculations might verify nonexponential polymer length distributions suggested by scaling arguments.[26] Also, this model could serve as a basis for understanding the dynamics of equilibrium polymers, possibly through a complex Langevin approach introduced by one of us.[10] This type of study has implications for understanding the rheological properties of micelle forming surfactant systems.[16]

Acknowledgment. The authors are grateful to the Dow Chemical Co. and the National Science Foundation (NSF-DMR-0312097) for supporting this research. We also thank V. V. Ginzburg for helpful discussions. E.H.F. thanks the Miller Institute at the University of California, Berkeley, for support during the preparation of this manuscript.

References and Notes

(1) Alexander-Katz, A.; Moreira, A. G.; Fredrickson, G. H. Field-theoretic simulations of confined polymer solutions. *J. Chem. Phys.* **2003**, *118*, 9030−9036.
(2) Bosman, A.; Brunsveld, L.; Folmer, B.; Sijbesma, R.; Meijer, E. Supramolecular polymers: From scientific curiosity to technological reality. *Macromol. Symp.* **2003**, *201*, 143−154.
(3) Cates, M. Dynamics of living polymers and flexible surfactant micelles—scaling laws for dilution. *J. Phys. (Paris)* **1988**, *49*, 1593.
(4) Cates, M.; Candau, S. Statics and dynamics of wormlike surfactant micelles. *J. Phys.: Condens. Matter* **1990**, *2*, 6869−892.
(5) de Gennes, P.-G. *Scaling Concepts in Polymer Physics*; Cornell University Press: Ithaca, NY, 1979.
(6) Dudowicz, J.; Freed, K. F.; Douglas, J. F. Lattice model of living polymerization. I. Basic thermodynamic properties. *J. Chem. Phys.* **1999**, *111*, 7116−7130.
(7) Dudowicz, J.; Freed, K. F.; Douglas, J. F. Lattice model of living polymerization. II. Interplay between polymerization and phase stability. *J. Chem. Phys.* **2000**, *112*, 1002−1010.
(8) Dudowicz, J.; Freed, K. F.; Douglas, J. F. Lattice model of living polymerization. III. Evidence for particle clustering from phase separation properties and "rounding" of the dynamical clustering transition. *J. Chem. Phys.* **2000**, *113*, 434−446.
(9) Ekani-Nkodo, A.; Kumar, A.; Fygenson, D. Joining and scission in the self-assembly of nanotubes from DNA tiles. *Phys. Rev. Lett.* **2004**, *93*, 268301.
(10) Fredrickson, G. H. Dynamics and rheology of inhomogeneous polymeric fluids: A complex Langevin approach. *J. Chem. Phys.* **2002**, *117*, 6810−6820.
(11) Fredrickson, G. H. *The Equilibrium Theory of Inhomogeneous Polymers*; Oxford University Press: New York, 2006.
(12) Fredrickson, G. H.; Ganesan, V.; Drolet, F. Field-theoretic computer simulation methods for polymers and complex fluids. *Macromolecules* **2002**, *35*, 16−39.
(13) Fredrickson, G. H.; Sides, S. W. Theory of polydisperse inhomogeneous polymers. *Macromolecules* **2003**, *36*, 5415−5423.
(14) Frigo, M.; Johnson, S. G. The design and implementation of FFTW3. *Proc. IEEE* **2005**, *93*, 216−231 (special issue on "Program Generation, Optimization, and Platform Adaptation").
(15) Greer, S. C. Reversible polymerizations and aggregations. *Annu. Rev. Phys. Chem.* **2002**, *53*, 173−200.
(16) Hu, Y.; Boltenhagen, P.; Pine, D. J. Shear thickening in low concentration solutions of wormlike micelles. I. Direct visualization of transient behavior and phase transitions. *J. Rheol.* **1998**, *42*, 1185−1208.
(17) Milchev, A. Phase transitions in polydisperse polymer melts. *Polymer* **1993**, *34*, 362−368.
(18) Milchev, A.; Landau, D. Adsorption of living polymers on a solid surface: A Monte Carlo simulation. *J. Chem. Phys.* **1996**, *104*, 9161−9168.
(19) Rouault, Y.; Milchev, A. A Monte Carlo lattice study of living polymers in a confined geometry. *Macromol. Theory Simul.* **1997**, *6*, 1177−1190.
(20) Ruokolainen, J.; Mäkinen, R.; Torkkeli, M.; Mäkelä, T.; Serimaa, R.; ten Brinke, G.; Ikkala, O. Switching supramolecular polymeric materials with multiple length scales. *Science* **1998**, *280*, 557−560.
(21) Schmitt, V.; Lequeux, F.; Marques, C. Confinement of dilute solutions of living polymers. *J. Phys. II* **1993**, *3*, 891−902.

(22) Sijbesma, R.; Beijer, F.; Brunsveld, L.; Folmer, B.; Hirschberg, J. K.; Lange, R.; Lowe, J.; Meijer, E. Reversible polymers formed from self-complementary monomers using quadruple hydrogen bonding. *Science* **1997**, *278*, 1601.
(23) van der Gucht, J.; Besseling, N. Statistical thermodynamics of equilibrium polymers at interfaces. *Phys. Rev. E* **2002**, *65*, 051801.
(24) van der Gucht, J.; Besseling, N.; Fleer, G. Surface forces induced by ideal equilibrium polymers. *J. Chem. Phys.* **2003**, *119*, 8175−8188.
(25) van der Gucht, J.; Besseling, N.; Fleer, G. Equilibrium polymers at interfaces: Analytical self-consistent-field theory. *Macromolecules* **2004**, *37*, 3026−3036.
(26) Wittmer, J.; Milchev, A.; Cates, M. Dynamical Monte Carlo study of equilibrium polymers: Static properties. *J. Chem. Phys.* **1998**, *109*, 834−845.

MA052223L